

PROPERTIES OF GOETHITES OF VARYING CRYSTALLINITY

UDO SCHWERTMANN, PHILIPPE CAMBIER,¹ AND ENVER MURAD

Lehrstuhl für Bodenkunde, Technische Universität München
D-8050 Freising-Weihenstephan, Federal Republic of Germany

Abstract—Goethites were synthesized from ferrihydrite in 0.7 M KOH between 4° and 90°C. As temperatures increased, the goethite crystals became larger and of less domainic character, and surface areas decreased from 153 to 9 m²/g. Surface area, oxalate-soluble Fe to total Fe ratios, chemisorbed water, Mössbauer parameters, and dissolution rate in 6 M HCl at 25°C are particle-size controlled, whereas mean crystallite dimensions, *a*-dimension of the unit cell, differences between the two OH-bending modes, and dehydroxylation temperatures suggest the existence of a low-temperature (high-*a*-dimension) and a high-temperature (low-*a*-dimension) goethite, with a narrow transition range at a synthesis temperature of 40°–50°C. Hydrothermal treatment at 125°–180°C of a low-temperature goethite led to a healing of the multidomainic, microporous high-*a*-dimension goethite into a monodomainic low-*a*-dimension goethite of similar overall crystal size with the properties of a low-*a*-dimension goethite.

Kurzfassung—Goethite wurden aus Ferrihydrit durch Lagerung in 0,7 m KOH bei Temperaturen zwischen 4° und 90°C hergestellt. Mit zunehmender Synthesetemperatur wurden die Goethitkristalle größer und deren Domänen-Charakter weniger stark ausgeprägt, während die spezifische Oberfläche von 153 auf 9 m²/g abnahm. Spezifische Oberfläche, Fe_{ox}/Fe_{tot}-Verhältnis, adsorptiv gebundenes Wasser, Mößbauerparameter und Lösungsgeschwindigkeit in 6 m HCl bei 25°C erwiesen sich als teilchengrößenabhängig. Dagegen sprachen die mittlere Teilchengröße, *a*-Gitterdimension, Abstand der beiden OH-Knickschwingungen und die Dehydroxylierungstemperatur für die Existenz eines Tieftemperatur- (hohe *a*-Gitterdimension) und eines Hochtemperatur-Goethits (niedrige *a*-Dimension) mit einem engen Übergangsbereich bei Synthesetemperaturen zwischen 40–50°C. Hydrothermale Behandlung eines Tieftemperatur-Goethits zwischen 125–180°C bewirkte ein Verheilen des vieldomänigen, mikroporösen Hoch-*a*-Goethits zu einen eindomänigen Niedrig-*a*-Goethit von ähnlichen Gesamtmaßen der Kristalle mit den Eigenschaften eines Niedrig-*a*-Goethits.

Resumé—Une série de goethites a été synthétisée à partir de ferrihydrite évoluant en milieu 0,7 M KOH, à une température variable comprise entre 4° et 90°C. Pour une température croissante, la taille des particules croît, leur caractère polycristallin disparaît, la surface diminue de 153 à 9 m²/g. La surface, la quantité d'eau chimisorbée, les paramètres Mössbauer, et la vitesse de dissolution dans HCl 0,6 M sont contrôlés par le facteur taille des particules, tandis que les dimensions moyennes des domaines cohérents, le paramètre *a* de la maille, l'écart entre les fréquences de déformation des OH et la température de deshydroxylation reflètent l'existence de 2 types de goethites, synthétisées respectivement à basse et haute température, caractérisées respectivement par un paramètre *a* grand et petit. Le domaine de transition en température se situe vers 40°–50°C. Un traitement hydrothermal à 125°–180°C d'une goethite "basse température" soude les domaines à l'intérieur du volume global des particules, fait décroître le paramètre *a* et apporte ainsi toutes les propriétés d'une goethite "haute température," à l'exception du volume global des cristallites qui est conservé.

Key Words—Crystallinity, Dissolution, Goethite, Hydrothermal treatment, Iron, Unit-cell dimension, X-ray powder diffraction.

INTRODUCTION

Quantification of fine-grained minerals in soils and sediments is often complicated by a considerable variation in what is commonly called crystallinity. For practical X-ray powder diffraction (XRD) work, crystallinity is usually estimated from line broadening, which may be caused by small crystal size and/or by crystal disorder. In choosing a suitable standard it is therefore advisable to select one with XRD line widths similar to those of the unknown material. Crystallinity in this broad sense reflects growth conditions which, in turn, depend on the environmental conditions under

which the minerals form. It is therefore important to characterize crystallinity as thoroughly as possible.

Goethites (α -FeOOH) from soils have been shown to vary strongly in XRD line broadening (Kühnel *et al.*, 1974; Schwertmann, 1984a). For pure and Al-substituted synthetic goethites produced under a range of conditions, Schulze and Schwertmann (1984) and Murad and Schwertmann (1983) demonstrated that properties such as cell dimensions, infrared absorption frequencies, dehydroxylation temperature, and magnetic hyperfine fields can vary considerably, even at identical degrees of Al substitution (including zero substitution).

In the present report we describe a number of properties of a series of pure, unsubstituted goethites of widely varying crystallinity, caused by different synthesis temperatures. The variations of a number of

¹ On leave from Station de Science du Sol, INRA, F-78000 Versailles, France.

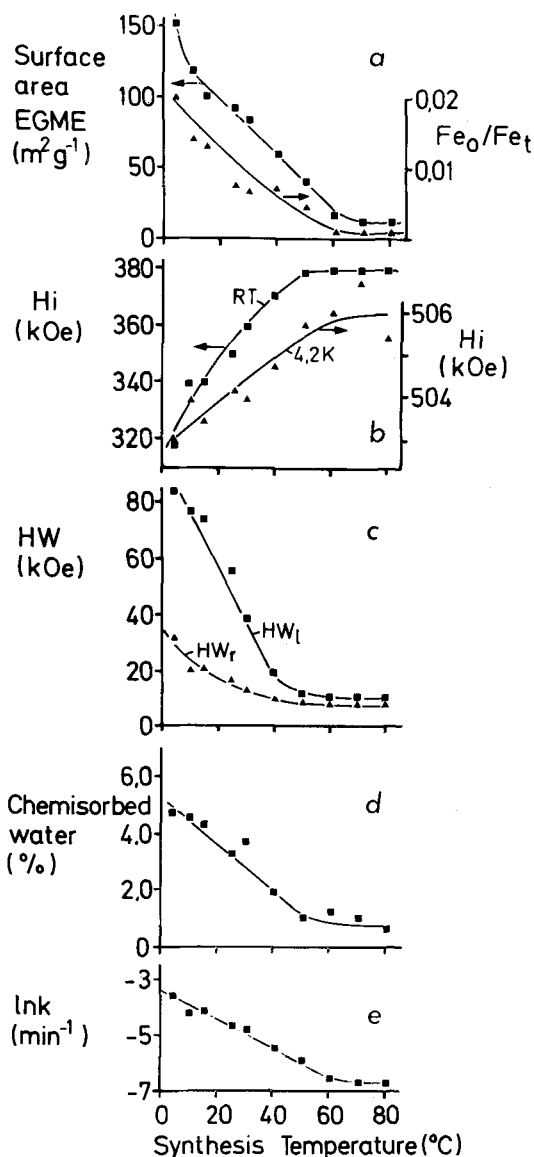


Figure 1. Change with synthesis temperature of surface-controlled properties of goethites of series 39/T. a. Surface areas and Fe_0/Fe_t ratios; b. Magnetic hyperfine fields at room temperature and 4.2°K; c. Half widths of hyperfine field distributions at room temperature; d. Chemisorbed water; e. Logarithm of dissolution rate constant.

physical properties are related to these differences in crystallinity.

MATERIALS AND METHODS

Sample preparation

Two series of goethites were prepared. For series 39/T, 50 ml of 1 M $Fe(NO_3)_3$ solution was added to 450 ml of KOH to yield a final $[OH^-]$ of 0.70 M. The suspensions were stored at various temperatures between 4° and 90°C for different lengths of time (Table

1) until an oxalate-soluble portion of less than 2% indicated essentially complete goethite formation. Once all ferrihydrite had been converted to goethite, variation of the storage duration caused no noticeable change in crystallinity, indicating that time was not a further independent variable. A second series (39/4T) was produced by treating the goethite formed at 4°C from series 39/T with water in a Teflon pressure vessel between 125° and 180°C. No hematite was formed by this treatment.

Instrumental techniques

X-ray powder diffraction was carried out using a Philips instrument with $CoK\alpha$ radiation and a diffracted-beam monochromator at a scanning speed of $1/2^\circ 2\theta/\text{min}$. The samples were backfilled and gently pressed against filter paper. The a , b , and c unit-cell dimensions were derived from the positions of the 110, 130, 111, and 140 lines using corundum as an internal standard. Line intensities were taken as products of heights multiplied by widths at half height. Mean crystallite dimensions were calculated from widths at half height corrected for instrumental line broadening (Schulze, 1984) using the Scherrer formula. For Mössbauer spectroscopy a $^{57}Co/Rh$ source was operated in a sinusoidal mode; spectra were taken at room temperature and 4.2°K with both source and absorber kept at identical temperatures. Room-temperature spectra were fitted with distributions of magnetic hyperfine fields as described by Murad (1982); 4.2°K spectra were taken using an iron foil as internal standard (Murad and Schwertmann, 1983; Murad, 1984). Infrared (IR) spectra were taken with 1:300 KBr pellets using a Beckman 4250 instrument at speeds of 150 and 20 cm^{-1}/min , the 1028.3- cm^{-1} band of polystyrene serving as standard. Where necessary, concentrations were adjusted by regrinding the pellets to obtain an absorbance of ≤ 0.65 for the δ_{OH} band at 890 cm^{-1} . Surface areas were determined by EGME adsorption (Carter *et al.*, 1965). Dissolution kinetics were studied using 6 N HCl at 25°C (Schwertmann, 1984b). Differential thermal analyses (DTA) were made of 50-mg samples with a Linseis DTA instrument at a heating rate of 10°C/min. Thermal gravimetric analyses (TGA) were made with a TGA Linseis instrument using 0.7 g samples and a heating rate of 5°C/min. Transmission electron microscopy (TEM) was carried out with a Zeiss EM 10 instrument. Oxalate-soluble Fe (Fe_0) and total Fe (Fe_t) were determined after extraction with acid oxalate (Schwertmann, 1964) and dissolution in concentrated HCl, respectively; Fe was determined by atomic absorption.

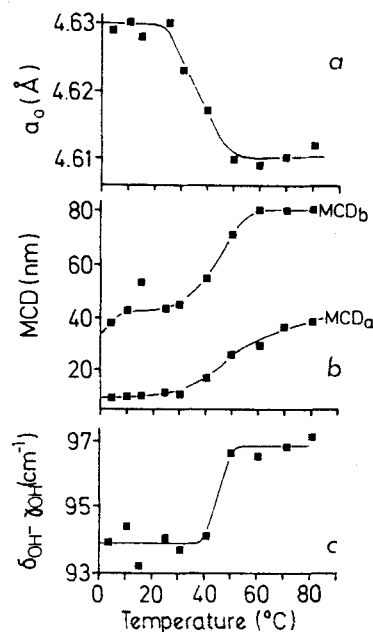
RESULTS AND DISCUSSION

Effect of synthesis temperature (series 39/T)

Mineralogy, surface area, and Fe_0/Fe_t ratio. All samples, with the exception of 39/80 and 39/90 (which

Table 1. Characteristics of goethites synthesized from ferrihydrite in 0.7 M KOH at various temperatures (series 39/T).

Synth. temp. (°C)	Dura- tion (days)	Fe _o /Fe _t × 10 ²	Surface area (m ² /g)	Weight loss (TGA)		Cell dimensions			MCD ₁₁₀ ² (Å)	MCD ₁₁₁ ² (Å)	I ₁₁₀ ³ /I ₁₁₁	IR absorption characteristics (cm ⁻¹)				Dissolution parameters				
				H ₂ O (%)	OH (%)	a (Å)	b (Å)	c (Å)				ν _{OH}	δ _{OH}	γ _{OH}	HAW ₉ ⁴	HAW ₆ ⁴	α	k · 10 ³ (min ⁻¹)		
4	68	2.0	153	4.74	10.98	4.629	9.959	3.025	90 (15)	380	1.38	3170	884.9	791.0	93.9	44.9	65.2	1.178	29	
10	35	1.4	119	4.57	11.09	4.629	9.946	3.027	100 (10)	430	1.64	3170	885.9	791.5	94.4	42.4	62.0	1.074	15	
15	28	1.3	101	4.34	12.00	4.628	9.955	3.025	105 (7)	530	1.59	3175	884.3	791.1	93.2	39.0	58.0	1.397	16	
25	13	0.78	92	3.28	10.68	4.630	9.947	3.024	111 (12)	430	2.66	3165	884.8	790.8	94.0	39.7	67.7	1.427	9.8	
30	13	0.69	85	3.79	10.90	4.623	9.959	3.027	112 (7)	450	3.41	3165	884.9	791.2	93.7	37.2	55.5	1.628	8.2	
40	13	0.75	60	2.08	11.29	4.617	9.953	3.025	162 (8)	540	4.60	3150	886.2	792.1	94.1	33.4	55.0	1.449	4.2	
50	13	0.47	41	1.01	10.69	4.610	9.955	3.025	260 (5)	710	3.86	3145	888.7	792.1	96.6	26.8	51.2	1.351	2.9	
60	7	<0.1	16	1.23	10.62	4.609	9.955	3.025	290 (30)	800	4.72	3150	889.2	792.7	96.5	24.3	50.4	1.352	1.4	
70	6	<0.1	13	0.94	10.71	4.610	9.955	3.024	360 (40)	800	4.41	3145	889.6	792.9	96.7	24.5	50.4	1.476	1.3	
80	7	<0.1	13	0.62	10.34	4.612	9.954	3.023	380 (20)	800	3.14	3145	890.5	793.4	97.1	24.3	49.2	1.429	1.3	
90	7	<0.1	9	n.d.	n.d.	n.d.	n.d.	n.d.	520 (60)	1080	3.44	3130	889.9	794.0	95.9	23.4	n.d.	n.d.	n.d.	n.d.

¹ Ratio of oxalate soluble Fe (Fe_o) to total Fe (Fe_t).² Mean crystallite dimension along [100] and [010] resp.; () = S.D.³ Diffraction intensity of 110 and 111.⁴ Half absorption width of δ_{OH} and the lattice vibration at 630 cm⁻¹.Figure 2. Change with synthesis temperature of structure-controlled properties of goethites of series 39/T. a. *a*-dimension; b. Mean crystal dimensions from XRD; c. Separation of OH-bending vibrations δ_{OH} - γ_{OH}.

contained a trace and about 10% hematite, respectively), consisted of pure goethite. The surface areas decreased more or less regularly from 153 m²/g at 4°C to 9 m²/g at 90°C (Figure 1a). The Fe_o/Fe_t ratios also decreased with increasing synthesis temperature, but were generally low indicating essentially complete conversion to goethite or goethite plus hematite. The Fe_o/Fe_t ratios increased with increasing surface area (Figure 1a), suggesting that the small amounts of Fe_o did not originate from residual ferrihydrite, but rather from surface zones of the goethite crystals. The variation of Fe_o/Fe_t ratios of synthetic goethites with surface area has been described by Schwertmann (1973).

Unit-cell dimensions. Schulze (1984) noted that the *a*-dimensions of unsubstituted goethites synthesized by different methods show a relatively large variation (from 4.608 and 4.629 Å). Similar variations were observed for the goethites studied here (Table 1). Figure 2a shows that *a* decreased as synthesis temperatures increased, although not in a regular fashion. It seems as though goethite can exist either as a "high-*a*-dimension" (*a* = 4.63 Å) or a "low-*a*-dimension" (*a* = 4.61 Å) modification, and that goethites with intermediate *a* values are rare. The latter goethites appeared to exist only in a narrow, intermediate formation-temperature range (30°–40°C), and seemed to be mixtures of the high-*a*-dimension and low-*a*-dimension modifications.

In contrast to the *a*-dimensions, the *b*- and *c*-di-

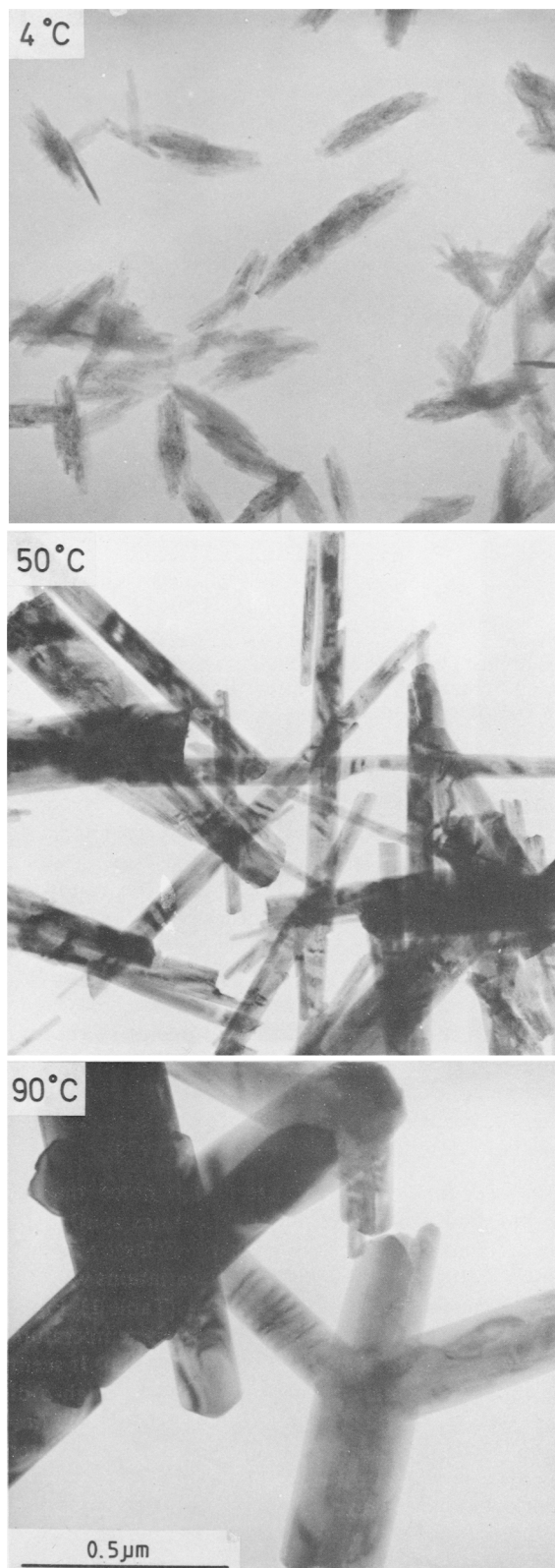


Figure 3. Electron micrographs of goethites synthesized at 4°, 50°, and 90°C.

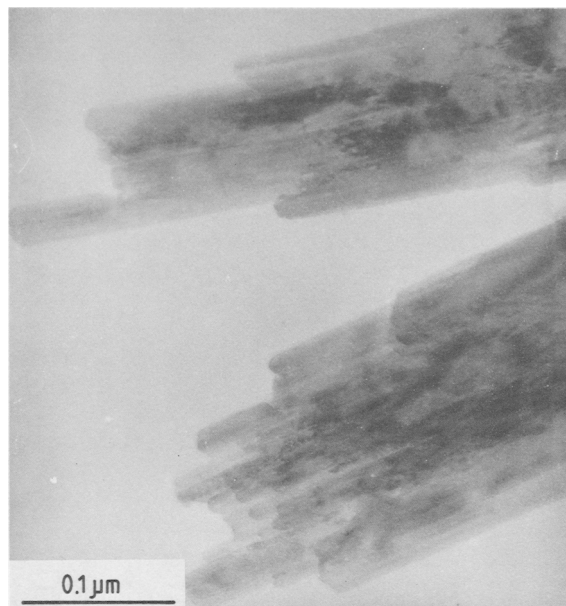


Figure 4. Electron micrograph of a multidomainic goethite crystal synthesized at 40°C.

mensions did not vary with formation temperature. This observation is in agreement with findings of Schulze (1984), and is attributed to the fact that the hydrogen bond, which is the weakest bond in the structure, has its largest vector in the *a*-direction, a smaller one in the *b*-direction, and no component in the *c*-direction.

X-ray diffraction intensities. The I_{110}/I_{111} ratio increased drastically up to a synthesis temperature of 40°C, but did not vary further at higher temperatures. This ratio reflects the degree of orientation of the acicular crystals parallel to the irradiated flat surface (Keller, 1967; Schulze and Schwertmann, 1984). The tendency for orientation increases with increasing size of the goethite needles. The wider scatter of data as the crystals become larger was therefore caused by the lack of reproducibility of the degree of orientation during preparation of the sample for XRD; the reproducibility depends in particular on the roughness of the surface against which the sample was (manually) pressed and the pressure applied. A comparison of I_{110}/I_{111} values of Table 1 with the calculated ratio given by Brindley and Brown (1980; Table 6.2) shows that orientation of the high-surface-area samples on the sample holder was negligible.

Crystal size and crystal morphology. Information about crystal size and morphology can be obtained from both X-ray diffraction line broadening (assuming this to be caused solely by the size of coherently scattering domains) and electron microscopy.

Mean crystallite dimensions (MCDs) were calculated

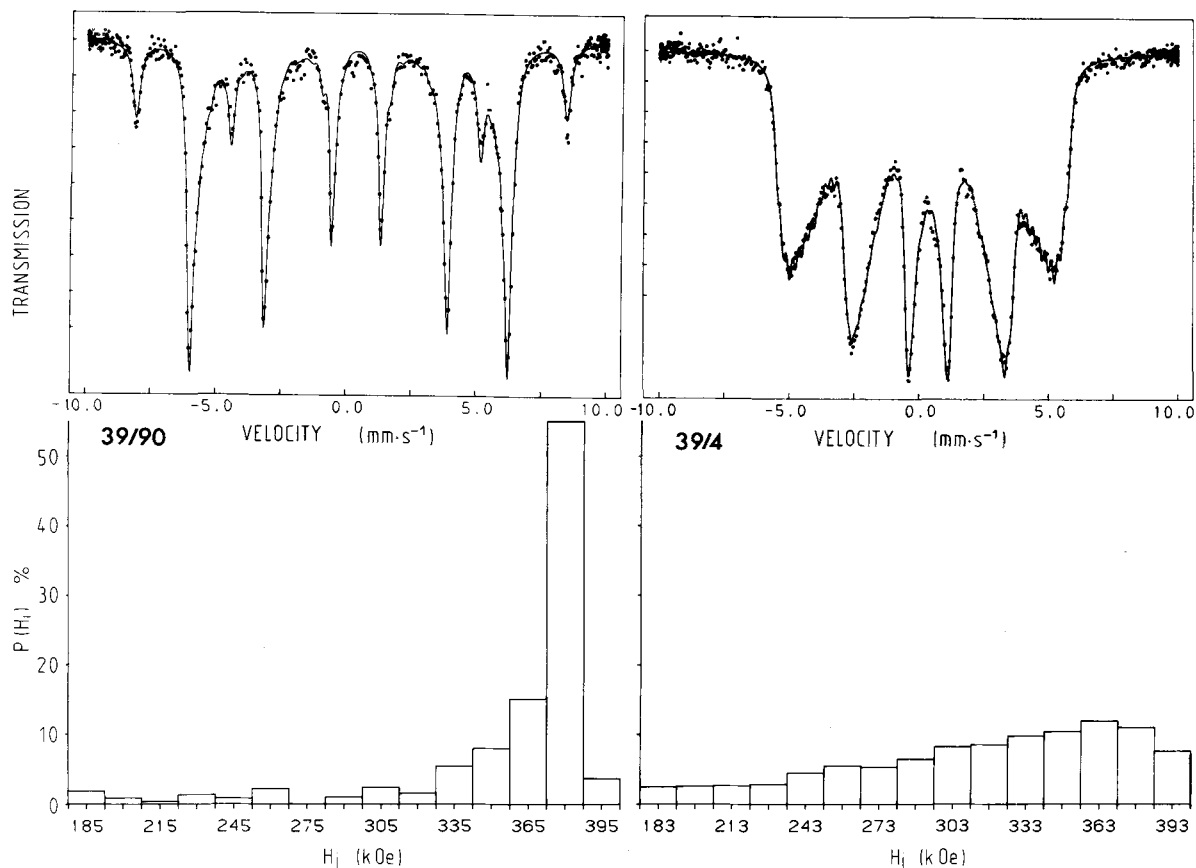


Figure 5. Room-temperature Mössbauer spectra fitted with distributions of magnetic hyperfine fields.

from the widths at half height of XRD lines using the Scherrer formula. The MCDs along the crystallographic axes were obtained from MCD_{hkl} values corrected with respect to the angle between the (hkl) plane and the respective axis. MCD_a (MCD parallel to the a -axis) was taken as the average value from the 110, 120, 130, 111, and 140 lines; the reasonably good agreement between these values (see SD in Table 1) indicates that line broadening was chiefly caused by small crystal size and not by disorder. Correspondingly, MCD_b was taken from the 020 and 021 lines. No suitable line is available to evaluate MCD_c (i.e., needle length), but the length can be readily estimated from EM observations.

As shown in Figure 2b, MCD_a was about 100 Å at <40°C synthesis temperature and increased to 300–400 Å at >60°C with an intermediate value at 50°C. The goethite produced at 90°C had a much higher MCD_a . A similar temperature dependence was observed for MCD_b , although all values were higher than MCD_a . MCD_b increased twofold from 400 Å at low temperature (with the exception of the 15°C sample) to 800 Å at high temperature. The goethite produced at 90°C had a much higher MCD_b . The “bimodal-

goethite” situation shown by the a unit-cell dimension was thus confirmed by the size of the coherently scattering X-ray domains.

Electron micrographs showed a strong dependence of crystal size and morphology on synthesis temperature. Between 4° and 40°C the crystals were polydomainic, the domains extending along [001] (Figure 3). The differences in domain lengths led to highly stepped crystal terminations (Figure 4). The widths of the domains, which may or may not terminate with well-developed (021) and (0 $\bar{2}$ 1) planes, were in the order of a few hundreds of Ångstrom units, which is slightly less than MCD_b (Table 1). The lengths of the crystals increased from 0.2–0.4 μm at 4°C to 0.5–1 μm at 30°C (Figure 2b). At 50°C the crystals were 1–2 μm long and 500–1000 Å wide, the latter value being in reasonable agreement with MCD_b (Table 1). Between 60° and 90°C an increasing proportion of mostly star-like twins developed. At 90°C the crystals had smooth edges and consisted of one—or at most a few—domains about 0.1 μm wide, again in agreement with the measured MCD_b values (Table 1). Twins were common at this temperature.

Thus, increasing synthesis temperature resulted in

Table 2. Mössbauer data for series 39/T and 39/4T goethites at room temperature and 4.2°K.

Sample	Room-temperature spectra					4.2°K spectra
	H _i ¹	FWHM ¹	H _{i,max} ²	HW _i ²	HW _r ²	H _i ¹
39/4	302	1.42	318	82	32	503.0
39/10	315	1.24	339	77	20	503.9
39/15	317	1.28	340	74	21	503.4
39/25	333	1.19	350	56	17	504.1
39/30	342	1.09	360	39	13	503.9
39/40	360	0.88	371	20	10	504.7
39/50	374	0.56	379	12	9	505.7
39/60	376	0.54	380	11	8	506.0
39/70	376	0.54	380	11	8	506.7
39/80	376	0.51	380	11	8	505.4
39/90	377	0.49	380	10	8	505.9
39/4 180 ³	376	0.56	381			505.1

¹ H_i, FWHM: Hyperfine fields and full line widths at half maximum for one-sextet fits.

² H_{i,max}, HW_i, HW_r: Hyperfine fields of maximum absorption, left (inner) and right (outer) half widths of hyperfine field distributions.

³ 7-day treatment.

crystals that were larger in all three directions and consisted of fewer and broader domains; it also enhanced twinning.

Magnetic properties as evidenced by Mössbauer spectroscopy. At room temperature all samples were completely magnetically ordered, giving Mössbauer spectra that comprised only one sextet (Figure 5). Simple one-sextet fits of these spectra indicated that magnetic hyperfine fields were essentially constant at about 376 kOe for samples synthesized between 90° and 50°C, and decreased linearly (Figure 1b) at a rate of about 1.5 kOe per degree lower synthesis temperature (Table 2). On the other hand, because of the asymmetric broadening of the resonant lines (FWHM 0.49 mm/sec for sample 39/90 to 1.42 mm/sec for sample 39/4, with a sudden increase from 0.56 to 0.88 mm/sec between samples 39/50 and 39/40), these fits offer at best a semi-quantitative assessment of the actual hyperfine fields. Such fits using a one-sextet model imply the existence of only one, well-defined magnetic hyperfine field. Wivel and Mørup (1981) and Murad (1982) showed that more realistic fits of room-temperature spectra of goethite can be obtained if distributions of hyperfine fields are implied. Fits carried out for hyperfine field distributions showed wide variations in the hyperfine fields of maximum absorption (H_{i,max}) and half widths of hyperfine field distributions (HW_i to the low-field side and HW_r to the high-field side of H_{i,max}) (see Figure 1c). These fits, in qualitative agreement with the results of the one-sextet fits, again showed little variation between synthesis temperatures of 90° and 4°C, followed by a decrease in H_{i,max} and considerable increases in the half widths of the hyperfine field distributions below 50°C. The higher variation of hy-

perfine fields given by one-sextet fits compared to that of H_{i,max} resulted from the fact that the former technique produced lines which were increasingly off the absorption maxima as these widened asymmetrically, i.e., they deviated increasingly from Lorentzian shape. This situation was also reflected in the variations of the half widths of the hyperfine field distributions: because of the asymmetric broadening of absorption maxima, the inner (lower-field) half widths increased much more strongly than the outer ones. This trend shows that, as synthesis temperatures decreased, the magnetic field came to contain increasing contributions from crystals of small particle size or otherwise poor crystallinity.

The 4.2°K spectra of samples 39/90 to 39/50 gave hyperfine fields averaging 505.9 ± 0.5 kOe, i.e., a value close to the maximum field found by Murad and Schwertmann (1983) for goethite of optimal crystallinity. The hyperfine field first decreased significantly to 504.7 kOe for sample 39/40, and continued to decrease more or less continuously as crystallinity decreased further. For the most poorly crystallized goethites 39/15 to 39/4, an average hyperfine field of 503.4 kOe was observed. In comparison, goethites of intermediate crystallinity produced by storing ferrihydrite in 2 M KOH at 70°C for 22 days (series 12; Murad and Schwertmann, 1983) gave a higher field of 504.1 kOe. Conversely, hydroxycarbonate goethite of the more poorly crystallized series 3+4 described in the same paper had a lower field of 500.0 kOe.

The variations of hyperfine fields at room temperature and 4.2°K and the widths of field distributions at room temperature paralleled the surface area, showing that these parameters are particle-size related.

Infrared absorption. As synthesis temperatures increased, the position of ν_{OH} (OH-stretching) shifted to smaller wave numbers, whereas the two OH-bending vibrations γ_{OH} and δ_{OH} shifted to larger wave numbers (Table 1). The lattice vibration at 640 cm⁻¹ (not given in Table 1) showed no definite trend. The position of δ_{OH}, however, shifted more than that of γ_{OH} and led to an increase in the difference δ_{OH} - γ_{OH}, which again showed a grouping at about 93-94 cm⁻¹ at 4°-40°C and 96-97 cm⁻¹ at 50°-80°C (Figure 2c). All bands furthermore became considerably narrower (as shown by their half absorption width, HAW) with increasing synthesis temperature.

The shifts of OH-vibration frequencies when crystallinity increases indicate an increasing strength of the OH...O bond (Pimentel and McClellan, 1960). This bond is not linear, but forms an angle in the *a-b* plane (Forsyth *et al.*, 1968). The vibration in the *a-b* plane, δ_{OH}, is therefore more affected than γ_{OH}, which is perpendicular to the *a-b* plane.

The increase of band widths as crystallinity decreased was not expected from an increasing H-bond

strength (Pimentel and McClellan, 1960), and thus seems to reflect randomly distributed structural defects. These results are not necessarily in contradiction with the XRD results, because IR spectroscopy tends to be more sensitive to a low degree of structural disorder than to higher disorder (Farmer, 1974, p. 195).

Dehydroxylation. As shown by Schwertmann (1984c), the DTA curves changed from a single low-temperature peak at 258°–278°C for samples 39/4–39/30, via a double peak (which was best developed at 50°C synthesis temperature), to a single, asymmetric high-temperature peak at 318°–320°C for samples 39/60–39/90. This shift suggests that, as with other properties, two types of goethites can also be deduced from the dehydroxylation behavior.

Unit-cell determinations and heating-stage XRD camera work of Schwertmann (1984c) on these samples showed the unit cell of the low-*a*-dimension goethite to shrink significantly in the *c* direction (e.g., from 3.023 to 2.994 Å for sample 39/50) before conversion to hematite, whereas the *b*-dimension was slightly dilated and the *a*-dimension remained unchanged. This low-*c*-dimension goethite is believed to have caused the higher dehydroxylation temperature. In contrast, the high-*a*-dimension goethite converted to hematite at a temperature too low to produce these changes in unit-cell size. Sample 39/50, containing both high- and low-*a*-dimension goethite, showed a double peak.

Surface water and structural OH. Thermogravimetric curves showed essentially two regions of weight loss above 80°C. The first weight loss occurred between about 80° and 160°C and is probably mainly due to chemisorbed surface water. This weight loss was followed by the main weight loss due to structural OH, which terminated at 500°C where a fairly constant weight was reached. The two weight losses were separated graphically from the intersection of the two extrapolated flatter parts of the curve.

The amount of structural OH lost ranged from 10.34 to 12.00% w/w (Table 1). This loss is slightly more than the theoretical weight loss of 10.14%, but was not related to synthesis temperature. In comparison, Paterson and Swaffield (1980) reported a weight loss of 11.8% for a synthetic goethite. The amount of chemisorbed water decreased with increasing synthesis temperature (Figure 1) and was closely related to specific surface area *S*:

$$\begin{aligned} \text{H}_2\text{O (mg/g)} &= 1.23 + 0.364S; \\ n &= 10; r = 0.964 \text{ (Figure 1d)}. \end{aligned}$$

From this relationship an average area of about 8 Å² per water molecule was calculated, which is slightly less than expected for a monolayer coverage (10 Å², Gast *et al.*, 1974).

Dissolution kinetics. As reported by Schwertmann

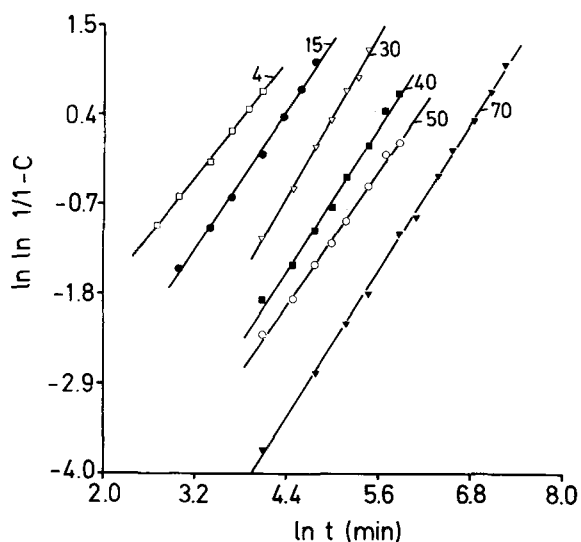


Figure 6. Linearized plot of dissolution vs. time curves. Goethites were dissolved in 6 M HCl at 25°C. Figures on the lines indicate synthesis temperature.

(1984b), multidomainic crystals show S-shaped dissolution-time curves in 6 M HCl at 25°C. The curves were attributed to preferential dissolution at the domain boundaries parallel to the needle axes, leading to an increase in surface area during the initial stages of dissolution.

The S-shaped dissolution curves can be mathematically described by Eq. (1) (Kabai, 1973):

$$C = 1 - e^{-Kt^\alpha}, \quad (1)$$

where *C* is the fraction of Fe dissolved at time *t*, and *K* and α are constants. Eq. (1) is an extended form of the pseudomonomolecular reaction equation, for which α becomes unity. *K* and α can be obtained from a linear transformation of Eq. (1):

$$\ln \ln 1/(1 - C) = \ln K + \alpha \ln t. \quad (2)$$

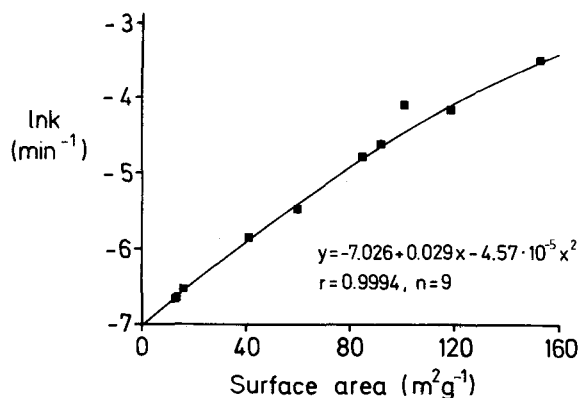


Figure 7. Relation between dissolution rate constant (min^{-1}) and surface area of goethites of series 39/T.

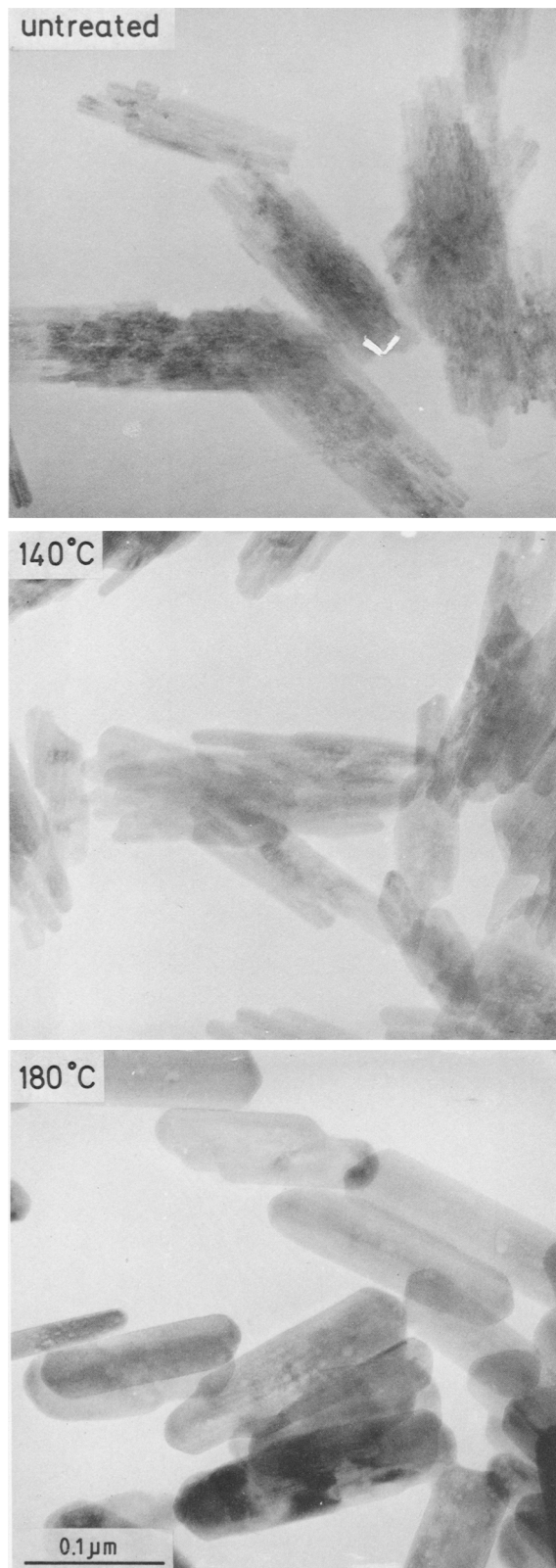


Figure 8. Electron micrographs of goethite synthesized at 4°C before and after hydrothermal treatment at 140° and 180°C for 16 hr.

Table 3. Characteristics of a goethite synthesized at 4°C before and after hydrothermal treatment at various temperatures for 16 hr (series 39/4T).

Temp. (°C)	$\text{Fe}_0\text{Fe}_t \times 10^2$	Surface area (m ² /g)	Cell dimensions			IR absorption characteristics (cm ⁻¹)						Dissolution parameters														
			$\frac{d_{110}}{d_{111}}$ (Å)	$\frac{d_{100}}{d_{111}}$ (Å)	$\frac{d_{010}}{d_{111}}$ (Å)	ν_{OH}	δ_{OH}	γ_{OH}	$\delta_{\text{OH}} - \gamma_{\text{OH}}$	HAW ₀ ⁵	Fe-O	α	$k \cdot 10^3$ (min ⁻¹)													
Untr. 39/4	2.2	153	4.629	9.959	3.025	MCD ₀ ² (Å)	90 (15)	MCD ₁ ² (Å)	380	$\frac{I_{110}^4}{I_{111}}$	1.38	ν_{OH}	3170	δ_{OH}	884.9	γ_{OH}	791.0	$\delta_{\text{OH}} - \gamma_{\text{OH}}$	93.9	HAW ₀ ⁵	44.9	Fe-O	641.1	α	1.178	29
125	0.66	66	4.619	9.945	3.025	148 (12)	530	1.89	3151	888.6	793.5	95.1	36.4	637.8	7.9											
140	0.56	53	4.616	9.950	3.025	184 (12)	480	1.79	3143	890.1	794.3	95.8	33.1	636.3	5.6											
160	0.54	45	4.611	9.952	3.025	210 (10)	560	1.89	3149	890.7	794.7	96.0	29.8	634.3	3.1											
180	0.52	52	4.612	9.943	3.024	280 (30)	640	1.95	3145	891.9	794.4	97.5	30.2	635.0	3.0											
180 ¹	0.20	34	4.607	9.960	3.024	330 (40)	680	1.72	3143	893.5	795.1	98.4	25.1	631.1	3.1											

¹ Treated for 7 days.

² Ratio of oxalate soluble Fe (Fe₀) to total Fe (Fe_t).

³ Mean crystallite dimension along 100 and 010, resp.

⁴ X-ray powder diffraction intensity of 110 and 111.

⁵ Half adsorption width of δ_{OH} .

The reaction rate constant k can be obtained from $\ln K = \alpha \ln k$ (Table 1). As seen from Figure 6, the experimental data are well described by Eq. (1), all correlation coefficients being $>.99$. Deviations occurred only at low dissolution times (not included), where the effective shaking period was underestimated because the filtration time was neglected. This held in particular for samples with a high dissolution rate.

The dissolution rate constant k decreased strongly with synthesis temperature between 4° and 60°C (Figure 1e). Above 60°C no further decrease was observed suggesting a highly significant relation between surface area and $\ln k$ (Figure 7), and indicating that the dissolution rate was largely surface-controlled.

For the dissolution of different metal oxides in various acids, Kabai (1973) suggested that α is characteristic of the structure of the solid phase, without, however, further specifying this suggestion. For our goethites, α varied only slightly and was not related to synthesis temperature (Table 2), thus supporting Kabai's (1973) hypothesis.

Partial dissolution resulted in an increase of $\delta_{\text{OH}} - \gamma_{\text{OH}}$. After 50% and 45% dissolution of samples 39/50 and 39/70, $\delta_{\text{OH}} - \gamma_{\text{OH}}$ increased from 96.6 to 100.7 cm^{-1} and from 96.7 to 101.6 cm^{-1} , respectively. If these changes reflect the strength of the H-bond, the goethite left after partial dissolution should have a slightly stronger H-bond, probably because of better crystallinity.

Effect of hydrothermal treatment on crystallinity (series 39/4 T). Table 3 summarizes the effect of a 16-hr treatment of sample 39/4 at 125° , 140° , 160° , and 180°C under water. Data for the untreated sample (39/4) are included for comparison. As expected, the hydrothermal treatment significantly improved crystallinity. This increase in crystallinity was reflected by an increase of MCD_a and MCD_b , the magnetic hyperfine fields at room temperature and 4.2°K , $\delta_{\text{OH}} - \gamma_{\text{OH}}$, and the dehydroxylation temperature (Schwertmann, 1984c). Conversely, Mössbauer line widths (Mössbauer spectra taken only for sample 39/4 180 in this sample set), surface area, chemisorbed water (for sample 39/4 180 from 4.74 to 0.85%), the a -dimension, dissolution rate, and Fe_0/Fe , decreased.

The dissolution rate constant k decreased with the temperature of hydrothermal treatment up to 160°C , above which no further decrease took place (Table 3). The values for the α -parameter were slightly higher than those of series 39/T (Table 1).

Electron micrographs (Figure 8) show that the crystals lost their serrated appearance with increasing hydrothermal temperature, until they finally developed smooth surfaces with a homogeneous interior. The overall crystal size, however, did not change, which is consistent with the low variation in I_{110}/I_{111} (Table 3). The drastic drop in specific surface area is somewhat

surprising in view of the unchanged overall size of the crystals. The higher initial surface is attributed to the serrated ends and longitudinal micropores between the domains of the untreated crystals, which would be accessible to EGME molecules used for surface area measurement. During the hydrothermal treatment, Fe must have dissolved from the serrated ends and reprecipitated in the micropores. Figure 7 shows that the serrated ends of the crystals first became rounded and then disappeared. These processes seem feasible because the exposed "ends" of the crystal are energetically less favorable positions than those in the micropores, which supply stable positions for crystal growth, provided the energy is sufficient for the Fe monomers to diffuse to these sites.

The disappearance of micropores and serrated ends is also in accord with a better agreement between the surface area calculated from overall crystal size with that determined experimentally by EGME and from chemisorbed water after the hydrothermal treatment. Before this treatment, the calculated surface area, using average width and length of the crystals from TEM and average thickness from XRD, yielded $62 \text{ m}^2/\text{g}$, a much lower value than the experimental EGME- and H_2O -surfaces of 153 and $177 \text{ m}^2/\text{g}$, respectively. After the hydrothermal treatment the calculated surface area was $28 \text{ m}^2/\text{g}$, which is much closer to the EGME- and H_2O -determined values of 34 and $32 \text{ m}^2/\text{g}$, respectively.

In contrast to observations of Sato *et al.* (1969), the position of the lattice vibration at 640 cm^{-1} moved to lower wave numbers as crystallinity improved (Table 3). These data are also different from the results of the temperature series 39/T (Table 1). The lattice vibration thus appears to be sensitive to crystallinity and crystal shape, both of which varied in the temperature series, whereas the hydrothermal treatment caused only crystallinity to vary.

CONCLUSIONS

The data show that goethites synthesized between 4° and 90°C varied in a number of properties. These properties may be tentatively divided into two groups: those that split the samples into two groups, and those that show a continuous variation with synthesis temperature.

The first group includes the a -dimension of the unit cell, the domain size in the a and b directions, the strength of the H-bond, and the dehydroxylation temperature. These properties appear to be structure-controlled, and both domain size and structural defects probably play a role. As the domain size was increased by hydrothermal treatment, all parameters varied accordingly. It is conceivable that below a certain domain size the a parameter of the unit cell increases, the H-bond weakens, and dehydroxylation takes place at a lower temperature. Schroerer and Nininger (1967) presented analogous data for hematite: the a -dimen-

sion increased by 2.1% as the crystal size decreased from 500 to 50 Å. Structural defects, randomly distributed over the whole crystal, may, however, have also caused a smaller domain size, a higher a -dimension, and a weaker H-bond at lower synthesis temperature.

The second group of properties, for which a more or less continuous variation with synthesis temperature was observed (surface area, Fe_o/Fe_t ratio, magnetic hyperfine field, chemisorbed water, and dissolution rate), may be related to crystal size, and therefore are surface-controlled. If the surface area is changed by "crystal healing," these parameters change accordingly.

Crystal properties such as those described in this paper probably reflect the growth conditions of a crystal. It therefore seems logical to use these as criteria to characterize the conditions of the environment in which weathering and goethite formation took place, as suggested by Kühnel *et al.* (1975), Schellmann (1983), and Schwertmann (1984a). Our preliminary results indeed showed a significant variation in the a -dimensions of goethites from various soil environments.

ACKNOWLEDGMENTS

We thank Mrs. B. Gallitscher and Ms. Ch. Wagner from the Lehrstuhl für Bodenkunde, Technische Universität München, for technical assistance, Dr. H.-Ch. Bartscherer, Physikalisches Institut of the T.U. München for the electron microscopic work, Dr. K. Kochloefl and Mr. O. Bock from the Girtler-Südchemie A.G., Moosburg, for supplying the thermal gravimetric analysis curves, Dr. R. M. Cornell, Institut für Anorganische Chemie, Universität Bern, for reading the manuscript, and the Deutsche Forschungsgemeinschaft for financial support.

REFERENCES

- Brindley, G. W. and Brown, G. (1980) *Crystal Structures of Clay Minerals and their X-ray Identification*: Mineralogical Society Monograph No. 5, London, 495 pp.
- Carter, D. L., Heilman, M. D., and Gonzales, C. L. (1965) The ethylene glycol monoethyl ether (EGME) technique for determining soil-surface area: *Soil Sci.* **100**, 409–413.
- Farmer, V. C. (1974) *The Infrared Spectra of Minerals*: Mineralogical Society Monograph No. 4, London, 539 pp.
- Forsyth, J. B., Hedley, I. G., and Johnson, C. E. (1968) The magnetic structure and hyperfine field of goethite (α -FeOOH): *J. Phys. C* **1**, 179–188.
- Gast, R. G., Landa, E. R., and Meyer, G. W. (1974) The interaction of water with goethite (α -FeOOH) and amorphous hydrated ferric oxide surfaces: *Clays & Clay Minerals* **22**, 31–39.
- Kabai, J. (1973) Determination of specific activation energies of metal oxides and metal oxide hydrates by measurement of the rate of dissolution: *Acta Chim. Acad. Sci. Hung.* **78**, 57–73.
- Keller, P. (1967) Quantitative röntgenographische Phasenanalyse verschiedener Rosttypen: *Werkst. Korr.* **18**, 865–878.
- Kühnel, R. A., Roorda, H. J., and Steensma, J. J. (1975) The crystallinity of minerals—a new variable in pedogenetic processes: a study of goethite and associated silicates in laterites: *Clays & Clay Minerals* **23**, 349–354.
- Murad, E. (1982) The characterization of goethite by Mössbauer spectroscopy: *Amer. Mineral.* **67**, 1007–1011.
- Murad, E. (1984) High-precision determination of magnetic hyperfine fields by Mössbauer spectroscopy: *J. Phys. E* **17**, 736–737.
- Murad, E. and Schwertmann, U. (1983) The influence of aluminium substitution and crystallinity in the Mössbauer spectra of goethite: *Clay Miner.* **18**, 301–312.
- Paterson, E. and Swaffield, R. (1980) Influence of adsorbed anions on the dehydroxylation of synthetic goethite: *J. Thermal Anal.* **18**, 161–167.
- Pimentel, G. C. and McClellan, A. L. (1960) *The Hydrogen Bond*: W. H. Freeman & Co., San Francisco, London, 475 pp.
- Sato, K., Sudo, T., Kurosawa, F., and Kammori, O. (1969) The influence of crystallization on the infrared spectra of α - and γ -ferric oxyhydroxides: *J. Japan Inst. Metals* **33**, 1371–1376.
- Schellmann, W. (1983) Geochemical principles of lateritic nickel ore formation: in *Proc. 2nd Int. Seminar Laterisation Processes, Sao Paulo, Brazil, 1982*. A. J. Melfi and A. Carvalho, eds., Instituto Astronomico e Geofisico, University of Sao Paulo, Brazil, 119–135.
- Schroeder, D. and Nininger, R. C. (1967) Morin transition in α -Fe₂O₃ microcrystals: *Phys. Rev. Lett.* **19**, 632–634.
- Schulze, D. G. (1984) The influence of aluminum on iron oxides. VIII. Unit-cell dimension of Al-substituted goethites and estimation of Al from them: *Clays & Clay Minerals* **32**, 36–44.
- Schulze, D. G. and Schwertmann, U. (1984) The influence of aluminium on iron oxides. X. The properties of Al-substituted goethites: *Clay Miner.* **19**, 521–539.
- Schwertmann, U. (1964) Differenzierung der Eisenoxide des Bodens durch photochemische Extraktion mit saurer Ammonium-oxalat-Lösung: *Z. Pflanzenernähr. Bodenk.* **105**, 194–202.
- Schwertmann, U. (1973) Use of oxalate for Fe extraction from soils: *Can. J. Soil Sci.* **53**, 244–246.
- Schwertmann, U. (1984a) The effect of pedogenetic environments on iron oxide minerals: *Adv. Soil Sci.* **1**, 171–200.
- Schwertmann, U. (1984b) The influence of aluminum on iron oxides. IX. Dissolution of Al-goethites in 6 M HCl: *Clay Miner.* **19**, 9–19.
- Schwertmann, U. (1984c) The double dehydroxylation peak of goethite: *Thermochim. Acta* **78**, 39–46.
- Wivel, C. and Mørup, S. (1981) Improved computation procedure for evaluation of overlapping hyperfine parameter distributions in Mössbauer spectra: *J. Phys. E* **14**, 605–610.

(Received 20 December 1984; accepted 28 April 1985; Ms. 1436)